J Mater Sci (2023) 58:1171–1182

Energy materials

High-performance supercapacitor and antifouling biosensor based on conducting polyaniline-hyaluronic acid hydrogels

Nianzu Liu[1,2], Yihui Ma[2], Zhenying Xu[2], Yingshu Guo[1,*], and Xiliang Luo[2,*]

[1] School of Chemistry and Chemical Engineering, Qilu University of Technology (Shandong Academy of Sciences), Jinan 250353, China

[2] Key Laboratory of Optic-Electric Sensing and Analytical Chemistry for Life Science, MOE, College of Chemistry and Molecular Engineering, Qingdao University of Science and Technology, Qingdao 266042, China

Received: 2 August 2022
Accepted: 1 December 2022
Published online:
14 December 2022

ABSTRACT

We report a polyaniline-hyaluronic acid (PANI-HA) hydrogel that combines rigid conducting polymer with flexible HA. The supramolecular assembly of PANI and HA via boronic acid bonds yields PANI-HA hydrogel with unique microstructure, electrical conductivity and hydrophilicity and exhibits excellent supercapacitor performance and electrochemical sensing for immunoglobulin G (IgG). The PANI-HA hydrogel electrode shows high specific capacitance (369 F g^{-1}, with 0.5 A g^{-1} current density) and good cycling stability (85% capacity retention after 1000 galvanostatic charge–discharge cycles). In addition, the PANI-HA hydrogel-based electrode can also be used as an electrochemical biosensor for IgG detection, and the presence of highly hydrophilic HA supports low-fouling target analysis. The modified electrode exhibits good sensitivity, wide detection range (0.1 ng mL^{-1}–10 μg mL^{-1}), and a low detection limit (0.043 ng mL^{-1}) for IgG detection. We demonstrate a strategy to fabricate supramolecular hydrogel-modified electrodes and explore their potential applications in supercapacitors and biosensors.

Handling Editor: Mark Bissett.

Address correspondence to E-mail: yingshug@126.com; xiliangluo@qust.edu.cn

https://doi.org/10.1007/s10853-022-08048-0

GRAPHICAL ABSTRACT

High-performance supercapacitor and antifouling biosensor were fabricated based on polyaniline-hyaluronic acid hydrogel.

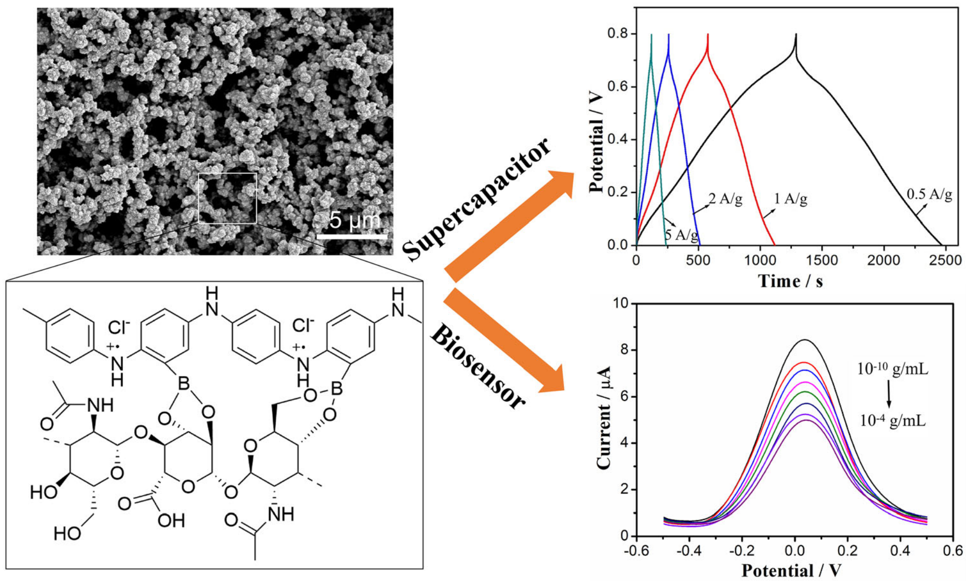

Introduction

In recent years, conducting polymer hydrogels have attracted great attention due to their high mechanical properties, low cost, and ease of synthesis [1–3]. Many supercapacitor devices based on conducting polymer hydrogels have emerged and also exhibit excellent energy storage properties [4–6]. Polyaniline (PANI) possesses distinct chemical properties, including simple doping mechanism, diverse and reversible redox behaviors, and high conductivity after protonation [7, 8]. As one of the commonly used conducting polymers, PANI conjugated π–electron skeleton has unique electrochemical properties, including high conductivity, reversibility between unique redox states and excellent biocompatibility [9, 10]. Its uncovered amino groups are susceptible to biomodification. Furthermore, the electrochemical characteristic peak signal of PANI corresponds to the transition of leucoemeraldine/emeraldine, which is extremely critical and useful in the field of electrochemical sensing [11, 12]. It has been used in many applications such as rechargeable batteries [13, 14], sensors [15–18], field effect transistors [19], catalytic supports [20–22] and supercapacitors [23, 24]. Bai et al. reported a pure PANI hydrogel synthesized by a fast in situ polymerization method, exhibiting high specific capacitance of 636 F g^{-1} and good cycling stability as a supercapacitor ($\sim$ 83% capacitance retention after 10,000 cycles) [25].

However, apart from capacitor efficiency, another neglected issue is the mechanical properties and long-term stability of the device [26]. The introduction of flexible polymer materials into rigid conducting polymer hydrogels is expected to enhance the long-term stability of the device while increasing the specific capacitance. For example, Liu et al. proposed a low-temperature polymerization strategy to prepare anisotropic polyvinyl alcohol/polyaniline (PVA/PANI) hydrogels [27]. Its high mechanical strength and bicontinuous phase structure achieve an extremely high energy density of 27.5 W h kg^{-1}. Ma et al. prepared a flexible solid-state supercapacitor based on PANI-PVA hydrogel with large capacity

(306 mF cm^{-2} and 153 F g^{-1}) [26]. This PANI-PVA hydrogel-based supercapacitor maintained about 100% capacity after 1000 mechanical folding cycles.

Another important application of these materials based on rigid conducting polymers and flexible polymers is to develop an antifouling electrochemical biosensor [28–30]. For example, PANI has been widely used in electrochemical sensing due to its high electrical conductivity, reversible redox behavior, and abundant doping mechanisms [11, 12, 31]. However, the practical applications of low-cost and fast-response electrochemical biosensors were limited, due to the severe biofouling in complex biological environments [32–34]. Proteins can non-specifically attach to the electrode surface, resulting in loss of sensitivity and reduced accuracy. Many antifouling materials have emerged to resist non-specific adsorption by providing highly hydrophilic and electrically neutral interfaces, such as polyethylene glycol (PEG) [35, 36], hyaluronic acid (HA) [37, 38], zwitterionic polymers [39, 40], peptides [11, 12], etc. Among them, HA is a hydrophilic anionic polysaccharide rich in carboxyl and hydroxyl groups, and its high hydrophilicity is capable of resisting non-specific protein adsorption [41]. Indeed, combining the unique electrical properties of PANI with the soft HA promises some tantalizing possibilities.

In this work, we choose HA as the soft material and conducting polymer PANI as the rigid polymer to improve structural stability and electrical conductivity of the hydrogel. The boronic acid groups can crosslink HA and PANI to form PANI-HA hydrogels [26]. PANI-HA hydrogels are supramolecular assembly at the molecular level via APS as an oxidant. The PANI-HA hydrogel was in situ gelled on the glassy carbon electrode (GCE) and modified with 5% Nafion solution to adhesive the material. We fabricated a supercapacitor based on this conducting polymer hydrogel with large electrochemical capacitance (369 F g^{-1}, with 0.5 A g^{-1} current density), outperforming other reported supercapacitors. Moreover, considering the high hydrophilicity and biocompatibility of the PANI-HA hydrogel, it helps to resist non-specific protein adsorption and provide an appropriate microenvironment for biomolecular recognition. An antifouling electrochemical biosensor based on PANI-HA hydrogel was constructed for detecting immunoglobulin G (IgG). This IgG sensing system shows a wide detection range (0.1 ng mL^{-1}–10 μg mL^{-1}) and low detection limit (0.043 ng mL^{-1}). We demonstrate the potential application of the prepared hydrogels in supercapacitor and biosensor with satisfactory performance, which provides a new idea for the application of conducting polymer-based flexible hydrogels.

Materials and methods

Chemicals

All reagents used in this work were of analytical grade. 3-Aminophenylboronic acid hydrochloride (ABA), hyaluronic acid (HA), 4-(N-Maleimidomethyl)cyclohexane-1-carboxylic acid 3-sulfo-N-hydroxysuccinimide ester sodium salt (sulfo-SMCC), and Nafion solution were purchased from Sigma-Aldrich. Aniline (AN), ammonium persulfate (APS), and hydrochloric acid (HCl) were obtained from Sinopharm Chemical Reagent Co., Ltd. Peptide aptamer (CHWRGWVA) were synthesized and purified by Hefei Bank-peptide Biological Technology Co., Ltd., in which the -HWRGWVA has been reported to specifically recognize IgG, and the terminal cysteine (C–) is used for anchoring [12, 32, 42]. IgG, human serum albumin (HSA) and other proteins were supplied by Shanghai Sangon Biotech Co., Ltd.

Apparatus

The morphology of the PANI hydrogel and PANI-HA hydrogel electrode were characterized by scanning electron microscope (SEM) (JEOL JSM-7500F, Hitachi High-Technology Co., Ltd.). Fourier-transform infrared spectroscopy (FTIR) (Nicolet iS20, Thermo Scientific Co., Ltd.), thermogravimetry (TGA) (TA Q50, TA Instruments Co., Ltd), and X-ray diffraction (XRD) (MinFlex 600, Rigaku Co., Ltd.) characterizations were performed to discuss the composition, structure, and properties of pure PANI, PANI hydrogel, and PANI-HA hydrogel. Static water contact angle (WCA) was used to measure the wettability of hydrogel-modified electrodes (JC2000D1, Shanghai Zhongchen Instrument Co., Ltd). All electrochemical measurements in this work were performed at room temperature using a CHI 660E Electrochemical Workstation (Shanghai CH Instrument Co., Ltd.).

Synthesis of PANI-HA and PANI hydrogel

0.48 mL 0.06 mM aniline and 0.32 mL 2 mM APS were cooled to 0 °C and then were rapidly mixed and reacted for 6 h at 4 °C to obtain pure PANI. The cooled 0.48 ml mixed solution containing 0.06 mM aniline, 0.004 mM ABA, and 0.2 mM HCl were quickly mixed with the cooled 0.32 mL 2 mM APS and reacted for 6 h at 4 °C to yield PANI hydrogel. The cooled 0.48 ml mixed solution containing 0.06 mM aniline, 0.004 mM ABA, and 0.2 mM HCl was quickly mixed with 0.2 mL 4 mg mL^{-1} HA and cooled 0.32 mL 2 mM APS, and then reacted for 6 h at 4 °C to obtain PANI-HA hydrogel.

Preparation of PANI-HA hydrogel and PANI hydrogel-modified electrodes.

During the gelation process, before the hydrogel was completely formed, 5 µL mixed solution was added onto the clean glassy carbon electrode (GCE). Then, 5 µL of ethanol-dispersed 5% Nafion solution was added onto the electrode surface. Electrodes modified with PANI-HA hydrogel (PANI-HA hydrogel electrodes) were successfully prepared by placing the modified electrode in the reaction at 4 °C for 6 h. The preparation process of electrodes modified with PANI hydrogel (PANI hydrogel electrodes) is similar, except that there is no HA mixed in the gelation process. Finally, the hydrogel-based electrodes were immersed in PBS (0.2 M, pH 7.4) for 6 h to remove impurities.

Electrochemical measurement of supercapacitor

The supercapacitor performance of the modified electrodes was performed on a CHI 660E workstation based on a conventional three-electrode system (working, reference, and counter electrode are PANI-HA hydrogel or PANI hydrogel-based electrode, Ag/AgCl electrode, and platinum wire, respectively) at room temperature. Its performance was characterized by cyclic voltammetry (CV), galvanostatic charge–discharge (GCD) tests. CV measurements were performed in the potential range of -0.2 to 0.8 V at a scan rate of 10–200 mV s^{-1} in 0.5 M $HClO_4$. The GCD measurements were conducted by sweeping from 0 to 0.8 V at current densities of 0.5 A g^{-1}–30 A g^{-1} in 0.5 M $HClO_4$ [26, 43].

Construction of PANI-HA hydrogel-based antifouling electrochemical biosensor

As shown in Fig. 4a, PANI-HA hydrogel electrodes were immersed in 2 mM sulfo-SMCC for 1 h and then incubated with peptide aptamer for 1 h. As a dual-activator, sulfo-SMCC binds the amino group on PANI to the sulfhydryl group on the cysteine terminal of the peptide, thereby modifying the peptide aptamer to the sensing interface [11, 12]. Finally, the obtained biosensing interface was rinsed repeatedly with DI water before use.

Antifouling and sensing of the electrochemical biosensor

The non-specific adsorption of interfering proteins at electrode interface was reflected by soaking the PANI-HA hydrogel and PANI hydrogel electrodes in different concentrations of HSA for 1 h. The peak current changes were recorded before and after soaking the protein. For detection of target molecules, the peptide/PANI-HA hydrogel electrodes were recruited in specific concentrations of IgG for 60 min, followed by repeated rinses with DI water. The signal response was measured by differential pulse voltammetry (DPV) in the range of − 0.5 to 0.5 V.

Electrochemical measurement of biosensor

The sensing performance of the PANI-HA hydrogel electrode was also performed based on a traditional three-electrode system (working, reference and counter electrodes are peptide/PANI-HA hydrogel electrode, Ag/AgCl electrode and platinum wire, respectively) at room temperature. DPV was used to record biosensor response data with potential increment of 4.0 mV and an amplitude of 50 mV. Signal suppression (%) shows the ratio of peak current changes before and after target recognition (Signal suppression (%) = $(i_{blank} - i_{target})/i_{blank} \times 100$).

Results and discussion

Material characterization

During the PANI-HA hydrogel synthesis, aniline was first copolymerized with ABA to form PANI with boronic acid group (Fig. 1a), and then the hydrogel

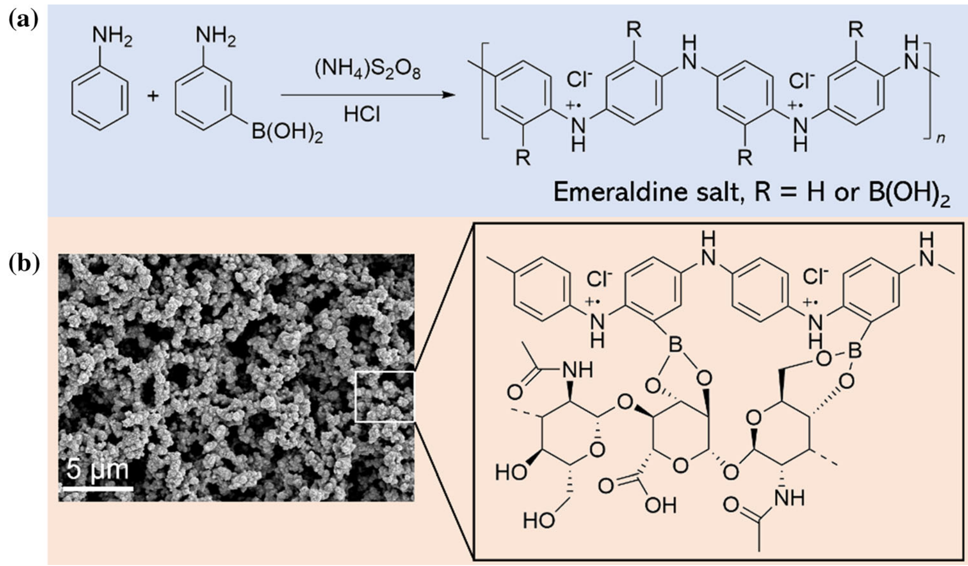

Figure 1 **a** Synthesis of PANI-bearing boronic acid groups. **b** A schematic molecular structure of PANI-HA hydrogel showing the crosslink between PANI and HA.

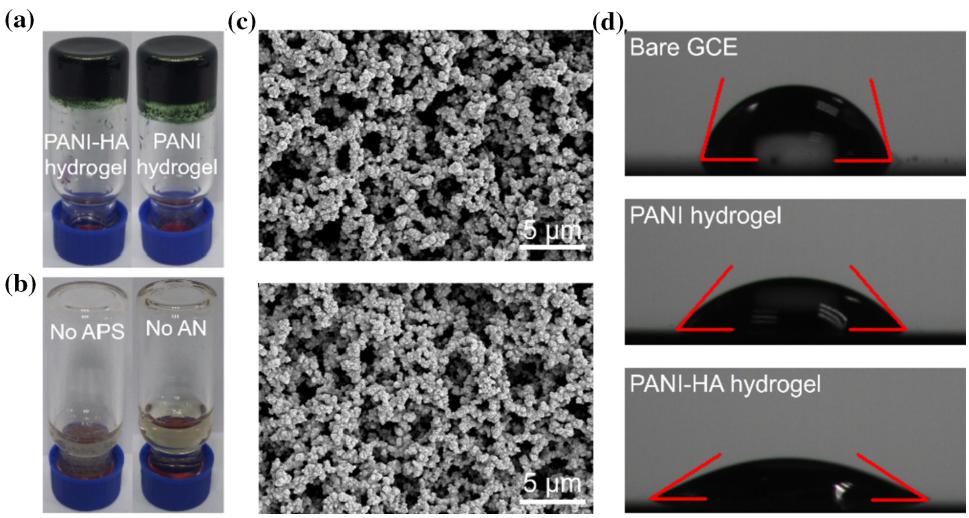

Figure 2 **a** Photograph of PANI-HA hydrogel and PANI hydrogel. **b** Pictures of reactions with different reagents. Vial 1 has no APS; vial 2 has no AN. SEM image of PANI-HA hydrogel **c** and PANI hydrogel **d** showing the porous structure. **e** Static water contact angles of bare GCE, PANI hydrogel and PANI-HA hydrogel-modified electrode. Bare GCE: 75.65°, PANI hydrogel electrode: 49.26°, PANI-HA hydrogel electrode: 32.25°.

was synthesized through the intermolecular interaction between the boronic acid group on PANI and the hydroxyl group on HA (Fig. 1b) since HA can undergo gelation in the presence of boric acid [44]. Furthermore, the boronic acid groups on ABA can copolymerize with aniline and thus covalently bind to PANI. As shown in Fig. 2a, the synthesized PANI hydrogel and PANI-HA hydrogel rapidly formed a dark green hydrogel within few minutes. The gelation process of PANI hydrogel and PANI-HA hydrogel in the first minute was recorded in Fig. S1. As shown in Fig. 2b, the hydrogel state cannot be synthesized without aniline and APS, indicating the necessity of aniline and APS in the synthesis process. The microscopic morphologies of the freeze-dried PANI hydrogel and PANI-HA hydrogel were then characterized by scanning electron microscopy (SEM). As shown in Fig. 2c, d, both hydrogels are composed of stacked spherical particles with a size of 10 nm and exhibit a porous network nanostructure. Furthermore, PANI-HA hydrogel possesses more abundant pores than PANI hydrogel, which is attributed to the looser structure provided by the high molecular weight HA as the flexible unit in the hydrogel [45]. Moreover, the properties of HA rich in polar groups lead to its easy binding to water molecules through ion solvation, thus forming a porous structure [46]. Conducting polymer network structures with high porosity are expected to improve interfacial conductivity and supercapacitor performance. The pure PANI (without boronic acid groups), PANI hydrogel and PANI-HA hydrogel were characterized by FTIR. As shown in Fig. S2, peaks around 1560 and 1480 cm^{-1} correspond to vibrations of the benzene ring in PANI [47]. Furthermore, the peak around 800 cm^{-1} is assigned to B–O vibration [48]. Peak at 1236 cm^{-1} in the PANI-HA hydrogel corresponds to the expansion vibration of C–O, and the peak at 1020 cm^{-1} corresponds to the expansion vibration of C–O–C [26]. As displayed in Fig. S3, the XRD plots of pure PANI (without boronic acid groups), PANI hydrgoel and PANI-HA hydrogel show that peaks around 24° are assigned to PANI [49]. The peaks around 59° correspond to boronic acid, and one peak around 20° corresponding to HA [50], demonstrating that constructed PANI hydrogel and PANI-HA hydrogel present ordered structures at the nanoscale. As shown in Fig. S4, the water content of both PANI hydrogel and PANI-HA hydrogel samples was determined to be 42 wt% by thermogravimetry. We characterized the interfacial hydrophilicity by static water contact angle (WCA) test, as shown in Fig. 2e, the contact angle of bare electrode is 75.65°, showing hydrophobicity. The contact angle data of the PANI-HA hydrogel and PANI hydrogel electrodes illustrate high hydrophilicity, respectively, which is attributed to the high water retention and high hydrophilicity of the hydrogels. The HA-containing PANI hydrogel electrode exhibits a smaller contact angle, which is due to the fact that HA contains more polar groups, which can bind more water molecules to form a hydration layer to withstand the non-specific adsorption of interfering proteins. The hydrophilic environment also provides a highly biocompatible microenvironment for the identification.

Supercapacitor characterization

In order to study the electrochemical properties of the prepared hydrogels, the two hydrogels were in situ gelled on bare GCE, and sealed with 5% Nafion solution to prepare hydrogel electrodes. The PANI-HA hydrogel and PANI hydrogel electrodes were characterized by cyclic voltammetry (CV) and galvanostatic charge–discharge (GCD) technologies. Figure 3a shows the CV curves with PANI-HA hydrogel electrode and bare GCE, respectively. The PANI-HA hydrogel electrode displayed a rectangular CV curve, which is typical of electrochemical double-layer supercapacitors. As shown in Fig. S5, characteristic redox peaks of PANI were observed from CV curves on both hydrogel-based electrodes, indicating the transition of PANI between different redox states. Figures 3b, c and S6 exhibit the symmetrical GCD curves of the PANI-HA hydrogel and PANI hydrogel electrodes at different current densities, respectively, indicating that both electrodes have highly reversible charge–discharge behaviors. As shown in Fig. 3d, both electrodes show good rate performance, when the current density increases from 0.5 to 30 A g^{-1}. The specific capacitance of the PANI-HA hydrogel electrode is higher than that of the PANI hydrogel electrode in different current density ranges, which is attributed to the introduction of flexible HA into the conducting polymer hydrogel network, the provided high porosity and high specific surface area conductive skeleton improve the electrochemical properties. Furthermore, the specific capacitances of the PANI-HA hydrogel electrodes and PANI hydrogel electrodes were calculated from the GCD data in the range of 0.5–30 A g^{-1} current densities (Table S1). The capacitance of the PANI-HA hydrogel electrode measured at 0.5 A g^{-1} reaches 369 F g^{-1}, which is comparable to previously reported conducting polymer-based electrodes and even better than previous reports (Table S2).

It is believed that the expansion and contraction of conducting polymers during charge and discharge generally lead to poor long-term cycling stability [26]. As shown in Figures S7a, b, both the PANI-HA hydrogel electrode and PANI hydrogel electrode were scanned for 100 GCD cycles at a current density of 0.5 A g^{-1}, exhibited excellent electrochemical stability. Moreover, as shown in Figures S7c, d, after 1000 GCD cycles at a current density of 30 A g^{-1}, the capacity retentions of PANI-HA hydrogel electrode and PANI hydrogel electrode were 85% and 72.1%, respectively. The good electrochemical stability of the PANI-HA hydrogel electrode is attributed to the introduction of HA, which enhances the mechanical properties and anti-interference of the hydrogel structure, thereby supporting and protecting the PANI framework during expansion and contraction.

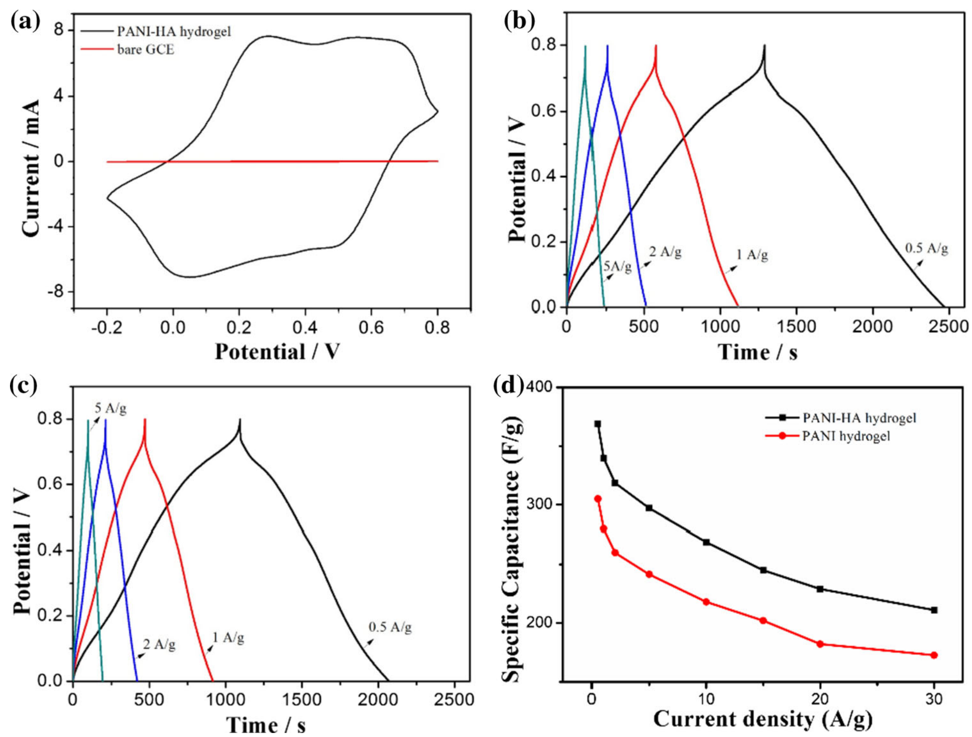

Figure 3 **a** CV plots of PANI-HA hydrogel electrode and bare GCE tested at a scan rate of 0.1 V s^{-1} in 0.5 M $HClO_4$ solution. GCD curves of **b** PANI-HA hydrogel electrode and **c** PANI hydrogel electrode in 0.5 M $HClO_4$ at different current densities solution (0.5, 1, 2, and 5 A g^{-1}). **d** Specific capacitance plots of PANI-HA hydrogel electrode and PANI hydrogel electrode at varied GCD current densities.

Antifouling performance

HA is a hydrophilic anionic polysaccharide rich in carboxyl and hydroxyl groups [41]. The flexible HA containing polar groups combined with the high water retention properties of hydrogel structure make the PANI-HA hydrogel electrodes highly hydrophilic to form a hydration layer to resist non-specific protein adsorption. In order to explore the possibility of constructing a sensing platform with PANI-HA hydrogel, the PANI-HA hydrogel-based electrodes were further covalently bound with peptides that could specifically recognize IgG proteins (Fig. 4a). As shown in Fig. 4b, the fabrication process of the sensing interface and the feasibility of the detection were characterized by differential pulse voltammetry (DPV) technology. The characteristic peak (47.3 μA) of the bare GCE appears around 0.15 V in 5.0 mM $[Fe(CN)_6]^{3-/4-}$ (curve a). After PANI-HA hydrogel was modified on the electrode (curve b), the PANI-HA hydrogel electrode exhibited a larger peak current (61.2 μA) in PBS (0.2 M, pH 7.4) at 0.07 V corresponding to the transition of standard redox forms of PANI [11, 31]. Large current response was attributed to the excellent conductive network provided by conducting polymer-based hydrogels. When the peptide was modified onto PANI-HA hydrogel electrode (curve c), the peak current decreased significantly (10.3 μA) due to the poor conductivity of the peptide. After incubation of the target IgG, specific recognition of proteins and peptides hinders charge transfer, resulting in a continued decrease (8.6 μA) in peak currents. The above results demonstrate the successful construction of the sensing interface.

Due to the excellent hydrophilicity of the PANI-HA hydrogel interface, the non-specific adsorption of proteins and cells can be effectively avoided. We explored and compared the antifouling properties of PANI-HA hydrogel electrodes and PANI hydrogel electrodes against different concentrations of human serum albumin (HSA). After incubation in HSA solution for 1 h, there were little signal change on PANI-HA hydrogel electrode (Fig. 4c). The signal suppression is shown in Fig. 4d; after the PANI-HA hydrogel electrode was soaked in 0.01 mg mL^{-1} HSA for 1 h, the signal only changed within 4%. Even after soaking in a high-concentration HSA (2 mg mL^{-1}), the signal suppression can also be controlled at about 10%, which is 36.5% suppressed compared to the PANI hydrogel electrode.

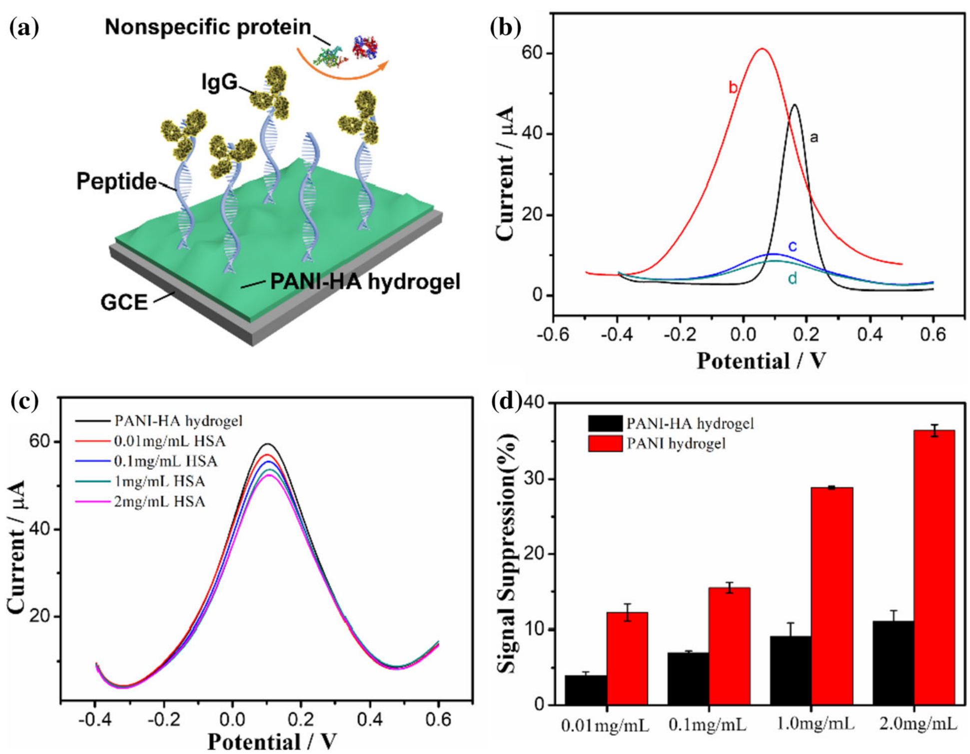

Figure 4 **a** Construction of an antifouling IgG biosensor based on PANI-HA hydrogel electrode for highly sensitive detection of IgG. **b** DPV curves corresponding to the electrode modification process (**a**: bare GCE in 5.0 mM $[Fe(CN)_6]^{3-/4-}$. **b**: PANI-HA hydrogel electrode, **c**: peptide/PANI-HA hydrogel electrode, and d: 1 ng mL^{-1} IgG/peptide/PANI-HA hydrogel electrode in PBS (0.2 M, pH 7.4)). **c** DPV curves of PANI-HA hydrogel electrode after soaking in different concentrations (0.01, 0.1, 1, and 2 mg mL.$^{-1}$) of HSA for 1 h. **d** Comparison of antifouling performance of PANI-HA hydrogel electrode (black column) and PANI hydrogel electrode (red column).

Determination of IgG

To obtain the optimal detection performance, we optimized the incubation time of the target IgG. As shown in Fig. S8, the signal suppression increased with the increasing incubation time, and the equilibrium was reached after 1 h of incubation time, indicating that the peptide binding to the target IgG reached saturation. Therefore, 1 h was chosen as the optimal incubation time.

Under optimal sensing conditions, we evaluate the sensing response of this antifouling electrochemical biosensor to IgG. The electroactive surface is continuously blocked with the increasing target concentration, resulting in a sequential decrease in peak current (Fig. 5a). The response range of the IgG biosensor is 0.1 ng mL^{-1}–10 μg mL^{-1}. The corresponding regression is signal suppression (%) = 5.325 log C (g mL^{-1}) + 63.99 (R^2 = 0.995) (Fig. 5b). The PANI-HA hydrogel-based electrochemical biosensor shows a lower limit of detection (LOD) of 0.043 ng mL^{-1} (S/N = 3), which is lower than many reported IgG sensors (Table S3). Such a lower LOD may be attributed to the high active surface area of PANI-HA hydrogel (producing a sensitive signal) and the brilliant biocompatibility of HA (offering a biocompatible microenvironment for the identification).

Specificity and stability of the biosensor

We selected high-concentration protein molecules (1 μg mL^{-1}) with different isoelectric points and different molecular weights as interfering proteins to explore the specificity of PANI-HA hydrogel electrodes. As shown in Fig. 5c, the electrochemical biosensor exhibited a greater current response to low concentrations of the target IgG (1 ng mL^{-1}), indicating excellent specificity. Moreover, we tested the long-term storage stability of the PANI-HA hydrogel electrode, and the results show that the signal retention was higher than 96% within 7 days

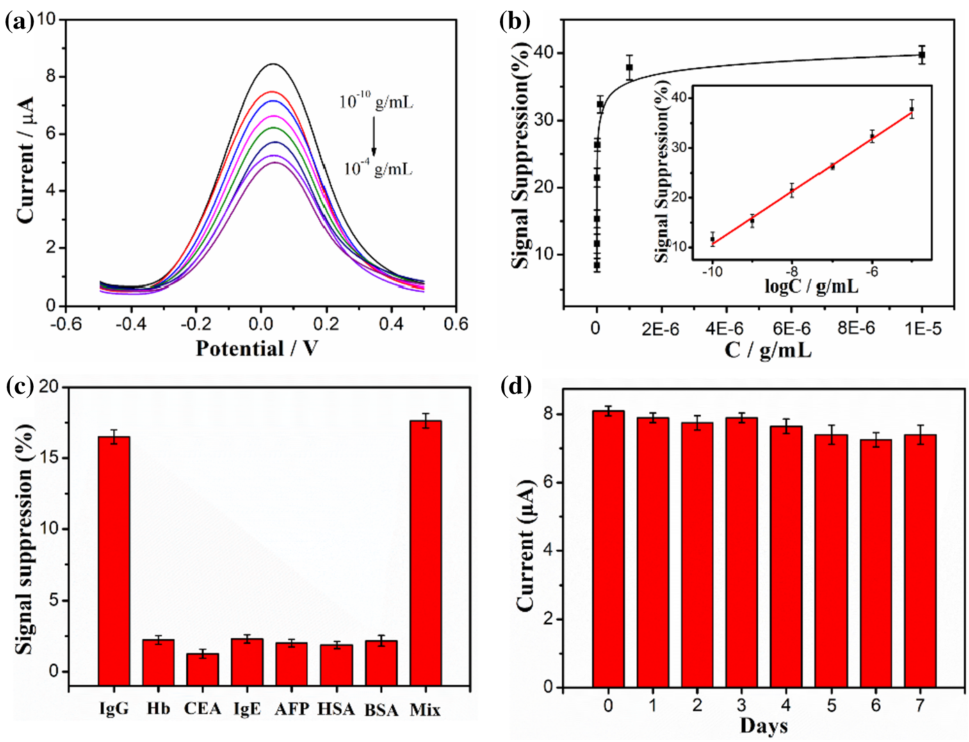

Figure 5 **a** DPV plots of the electrochemical biosensor to IgG. **b** The relationship between the peak current and the concentration after incubation with a specific IgG concentration in PBS (0.2 M, pH 7.4). Corresponding calibration plot is shown in the inset (R^2 = 0.995). **c** Signal responses of the electrochemical biosensor to 1 μg mL^{-1} of hemoglobin (Hb), carcinoembryonic antigen (CEA), immunoglobulin E (IgE), alpha fetoprotein (AFP), HSA, bovine serum albumin (BSA), and 1 ng mL^{-1} IgG, and a mixture (Mix) of proteins, respectively. **d** Long-term stability of the PANI-HA hydrogel interface over 7 days.

(Fig. 5d), indicating the possibility of its long-term application.

Conclusion

We have successfully prepared a PANI-HA hydrogel combining a rigid conducting polymer PANI and a soft polymer HA. In terms of supercapacitor performance, the PANI-HA hydrogel electrode shows a large specific capacitance and brilliant cycling stability compared to the pure PANI hydrogel, which is attributed to the increased porosity and specific surface area of PANI-HA hydrogel. In addition, PANI-HA hydrogel-based electrode can achieve an antifouling interface due to the presence of highly hydrophilic HA. The prepared biosensing platform based on PANI-HA hydrogel also exhibited good sensitivity, wide detection range, and low detection limit for IgG detection. We provide a new idea for the application of conducting polymer-based flexible hydrogels.

Acknowledgements

We acknowledge the financial support of the National Natural Science Foundation of China (21974075) and the Taishan Scholar Program of Shandong Province of China (ts20110829)

Declarations

Conflicts of interest The authors declare that there is no conflict of interest in this paper.

Supplementary Information: The online version contains supplementary material available at https://doi.org/10.1007/s10853-022-08048-0.

References

[1] Ma Z, Shi W, Yan K, Pan L, Yu G (2019) Doping engineering of conductive polymer hydrogels and their application in advanced sensor technologies. Chem Sci 10:6232–6244. https://doi.org/10.1039/C9SC02033K

[2] Tomczykowa M, Plonska-Brzezinska ME (2019) Conducting Polymers, hydrogels and their composites: preparation, properties and bioapplications. Polymers 11:350–386. https://doi.org/10.3390/polym11020350
[3] Zeng R, Wang W, Chen M, Wan Q, Wang C, Knopp D, Tang D (2021) CRISPR-Cas12a-driven MXene-PEDOT:PSS piezoresistive wireless biosensor. Nano Energy 82:105711–105738. https://doi.org/10.1016/j.nanoen.2020.105711
[4] Han X, Xiao G, Wang Y et al (2020) Design and fabrication of conductive polymer hydrogels and their applications in flexible supercapacitors. J Mater Chem A 8:23059–23095. https://doi.org/10.1039/D0TA07468C
[5] Wang Y, Ding Y, Guo X, Yu G (2019) Conductive polymers for stretchable supercapacitors. Nano Res 12:1978–1987. https://doi.org/10.1007/s12274-019-2296-9
[6] Li P, Jin Z, Peng L, Zhao F, Xiao D, Jin Y, Yu G (2018) Stretchable all-gel-state fiber-shaped supercapacitors enabled by macromolecularly interconnected 3D graphene/nanostructured conductive polymer hydrogels. Adv Mater 30:1800124–1800131. https://doi.org/10.1002/adma.201800124
[7] Li G, Zhong P, Ye Y, Wan X, Cai Z, Yang S, Xia Y, Li Q, Liu J, He Q (2019) A highly sensitive and stable dopamine sensor using shuttle-like α-Fe_2O_3 nanoparticles/electro-reduced graphene oxide composites. J Electrochem Soci 166:1552–1562. https://doi.org/10.1149/2.1071915jes
[8] Bhadra S, Khastgir D, Singha NK, Lee JH (2009) Progress in preparation, processing and applications of polyaniline. Prog Polym Sci 34:783–810. https://doi.org/10.1016/j.progpolymsci.2009.04.003
[9] Ren R, Cai G, Yu Z, Zeng Y, Tang D (2018) Metal-polydopamine framework: an innovative signal-generation tag for colorimetric immunoassay. Anal Chem 90:11099–11105. https://doi.org/10.1021/acs.analchem.8b03538
[10] Zeng R, Luo Z, Zhang L, Tang D (2018) Platinum nanozyme-catalyzed gas generation for pressure-based bioassay using polyaniline nanowires-functionalized graphene oxide framework. Anal Chem 90:12299–12306. https://doi.org/10.1021/acs.analchem.8b03889
[11] Liu N, Song J, Lu Y, Davis JJ, Gao F, Luo X (2019) Electrochemical aptasensor for ultralow fouling cancer cell quantification in complex biological media based on designed branched peptides. Anal Chem 91:8334–8340. https://doi.org/10.1021/acs.analchem.9b01129
[12] Liu N, Hui N, Davis JJ, Luo X (2018) Low fouling protein detection in complex biological media supported by a designed multifunctional peptide. ACS Sens 3:1210–1216. https://doi.org/10.1021/acssensors.8b00318
[13] Kim C, Ahn BY, Wei T-S et al (2018) High-power aqueous zinc-ion batteries for customized electronic devices. ACS Nano 12:11838–11846. https://doi.org/10.1021/acsnano.8b02744
[14] Xie J, Zhang Q (2019) Recent progress in multivalent metal (Mg, Zn, Ca, and Al) and metal-ion rechargeable batteries with organic materials as promising electrodes. Small 15:1805061–1805081. https://doi.org/10.1002/smll.201805061
[15] Liu C, Tai H, Zhang P, Yuan Z, Du X, Xie G, Jiang Y (2018) A high-performance flexible gas sensor based on self-assembled PANI-CeO_2 nanocomposite thin film for trace-level NH_3 detection at room temperature. Sens Actuators B 261:587–597. https://doi.org/10.1016/j.snb.2017.12.022
[16] Hou X, Zhou Y, Liu Y, Wang L, Wang J (2020) Coaxial electrospun flexible PANI//PU fibers as highly sensitive pH wearable sensor. J Mater Sci 55:16033–16047. https://doi.org/10.1007/s10853-020-05110-7
[17] Yu Z, Cai G, Liu X, Tang D (2021) Pressure-based biosensor integrated with a flexible pressure sensor and an electrochromic device for visual detection. Anal Chem 93:2916–2925. https://doi.org/10.1021/acs.analchem.0c04501
[18] Huang L, Zeng R, Tang D, Cao X (2022) Bioinspired and multiscale hierarchical design of a pressure sensor with high sensitivity and wide linearity range for high-throughput biodetection. Nano Energy 99:107376–107387. https://doi.org/10.1016/j.nanoen.2022.107376
[19] Amer K, Elshaer AM, Anas M, Ebrahim S (2019) Fabrication, characterization, and electrical measurements of gas ammonia sensor based on organic field effect transistor. J Mater Sci Mater Electron 30:391–400. https://doi.org/10.1007/s10854-018-0303-7
[20] Ahamad T, Naushad M, Alzaharani Y, Alshehri SM (2020) Photocatalytic degradation of bisphenol-A with g-C3N4/MoS2-PANI nanocomposite: kinetics, main active species, intermediates and pathways. J Mol Liq 311:113339–113349. https://doi.org/10.1016/j.molliq.2020.113339
[21] Chen Y, Zhang Q, Jing X, Han J, Yu L (2019) Synthesis of Cu-doped polyaniline nanocomposites (nano Cu@PANI) via the H_2O_2-promoted oxidative polymerization of aniline with copper salt. Mater Lett 242:170–173. https://doi.org/10.1016/j.matlet.2019.01.143
[22] Liu N, Wang R, Gao S et al (2021) High-performance piezo-electrocatalytic sensing of ascorbic acid with nanostructured wurtzite zinc oxide. Adv Mater 33:2105697–2105706. https://doi.org/10.1002/adma.202105697
[23] Qiu Z, Peng Y, He D, Wang Y, Chen S (2018) Ternary Fe3O4@C@PANi nanocomposites as high-performance supercapacitor electrode materials. J Mater Sci

53:12322–12333. https://doi.org/10.1007/s10853-018-2451-9
[24] Zhao X, Gnanaseelan M, Jehnichen D, Simon F, Pionteck J (2019) Green and facile synthesis of polyaniline/tannic acid/rGO composites for supercapacitor purpose. J Mater Sci 54:10809–10824. https://doi.org/10.1007/s10853-019-03654-x
[25] Zhou K, He Y, Xu Q et al (2018) A hydrogel of ultrathin pure polyaniline nanofibers: oxidant-templating preparation and supercapacitor application. ACS Nano 12:5888–5894. https://doi.org/10.1021/acsnano.8b02055
[26] Li W, Gao F, Wang X, Zhang N, Ma M (2016) Strong and robust polyaniline-based supramolecular hydrogels for flexible supercapacitors. Angew Chem Int Ed 55:9196–9201. https://doi.org/10.1002/anie.201603417
[27] Li L, Zhang Y, Lu H et al (2020) Cryopolymerization enables anisotropic polyaniline hybrid hydrogels with superelasticity and highly deformation-tolerant electrochemical energy storage. Nat Commun 11:62–74. https://doi.org/10.1038/s41467-019-13959-9
[28] Jiang X, Wang H, Yuan R, Chai Y (2018) Functional three-dimensional porous conductive polymer hydrogels for sensitive electrochemiluminescence in situ detection of H_2O_2 released from live cells. Anal Chem 90:8462–8469. https://doi.org/10.1021/acs.analchem.8b01168
[29] Yang L, Wang H, Lü H, Hui N (2020) Phytic acid functionalized antifouling conducting polymer hydrogel for electrochemical detection of microRNA. Anal Chim Acta 1124:104–112. https://doi.org/10.1016/j.aca.2020.05.025
[30] Huang L, Zeng R, Xu J, Tang D (2022) Point-of-care immunoassay based on a multipixel dual-channel pressure sensor array with visual sensing capability of full-color switching and reliable electrical signals. Anal Chem 94:13278–13286. https://doi.org/10.1021/acs.analchem.2c03393
[31] Liu N, Fan X, Hou H, Gao F, Luo X (2021) Electrochemical sensing interfaces based on hierarchically architectured zwitterionic peptides for ultralow fouling detection of alpha fetoprotein in serum. Anal Chim Acta 1146:17–23. https://doi.org/10.1016/j.aca.2020.12.031
[32] Liu N, Ma Y, Han R, Lv S, Wang P, Luo X (2021) Antifouling biosensors for reliable protein quantification in serum based on designed all-in-one branched peptides. Chem Commun 57:777–780. https://doi.org/10.1039/D0CC07220F
[33] Liu N, Xu Z, Morrin A, Luo X (2019) Low fouling strategies for electrochemical biosensors targeting disease biomarkers. Anal Methods 11:702–711. https://doi.org/10.1039/C8AY02674B
[34] Jiang C, Wang G, Hein R, Liu N, Luo X, Davis JJ (2020) Antifouling strategies for selective in vitro and in vivo sensing. Chem Rev 120:3852–3889. https://doi.org/10.1021/acs.chemrev.9b00739
[35] Hui N, Sun X, Niu S, Luo X (2017) PEGylated polyaniline nanofibers: antifouling and conducting biomaterial for electrochemical DNA sensing. ACS Appl Mater Interfaces 9:2914–2923. https://doi.org/10.1021/acsami.6b11682
[36] Zhi Z, Su Y, Xi Y et al (2019) Correction to "Dual-functional polyethylene glycol-b-polyhexanide surface coating with in vitro and in vivo antimicrobial and antifouling activities." J Mater Chem 11:15181–15181. https://doi.org/10.1021/acsami.9b05542
[37] Fan B, Fan Q, Cui M, Wu T, Wang J, Ma H, Wei Q (2019) Photoelectrochemical biosensor for sensitive detection of soluble CD44 based on the facile construction of a poly(ethylene glycol)/hyaluronic acid hybrid antifouling interface. ACS Appl Mater Interfaces 11:24764–24770. https://doi.org/10.1021/acsami.9b06937
[38] Parfenova LV, Galimshina ZR, Gil'fanova GU et al (2022) Hyaluronic acid bisphosphonates as antifouling antimicrobial coatings for PEO-modified titanium implants. Surf Interfaces 28:101678–101689. https://doi.org/10.1016/j.surfin.2021.101678
[39] Pan C, Chen L, Liu S, Zhang Y, Zhang C, Zhu H, Wang Y (2016) Dopamine-assisted immobilization of partially hydrolyzed poly(2-methyl-2-oxazoline) for antifouling and biocompatible coating. J Mater Sci 51:2427–2442. https://doi.org/10.1007/s10853-015-9556-1
[40] Wang C, Li Z, Chen J et al (2018) Influence of blending zwitterionic functionalized titanium nanotubes on flux and anti-fouling performance of polyamide nanofiltration membranes. J Mater Sci 53:10499–10512. https://doi.org/10.1007/s10853-018-2288-2
[41] Xia Y, Adibnia V, Shan C et al (2019) Synergy between zwitterionic polymers and hyaluronic acid enhances antifouling performance. Langmuir 35:15535–15542. https://doi.org/10.1021/acs.langmuir.9b01876
[42] Zhang Y, Carbonell RG, Rojas OJ (2013) Bioactive cellulose nanofibrils for specific human IgG binding. Biomacromol 14:4161–4168. https://doi.org/10.1021/bm4007979
[43] Hui N, Chai F, Lin P et al (2016) Electrodeposited conducting polyaniline nanowire arrays aligned on carbon nanotubes network for high performance supercapacitors and sensors. Electrochim Acta 199:234–241. https://doi.org/10.1016/j.electacta.2016.03.115
[44] Guan Y, Zhang Y (2013) Boronic acid-containing hydrogels: synthesis and their applications. Chem Soc Rev 42:8106–8121. https://doi.org/10.1039/C3CS60152H

[45] Wang L, Dong S, Liu Y et al (2020) Fabrication of injectable, porous hyaluronic acid hydrogel based on an in-situ bubble-forming hydrogel entrapment process. Polymers 12:1138–1153. https://doi.org/10.3390/polym12051138

[46] Ying H, Zhou J, Wang M, Su D, Ma Q, Lv G, Chen J (2019) In situ formed collagen-hyaluronic acid hydrogel as biomimetic dressing for promoting spontaneous wound healing. Mater Sci Eng C 101:487–498. https://doi.org/10.1016/j.msec.2019.03.093

[47] Lee J-E, Yamaguchi A, Ooka H, Kazami T, Miyauchi M, Kitadai N, Nakamura R (2021) In situ FTIR study of CO_2 reduction on inorganic analogues of carbon monoxide dehydrogenase. Chem Commun 57:3267–3270. https://doi.org/10.1039/D0CC07318K

[48] Saleem S, Sajid MS, Hussain D, Jabeen F, Najam-ul-Haq M, Saeed A (2020) Boronic acid functionalized MOFs as HILIC material for N-linked glycopeptide enrichment. Anal Bioanal Chem 412:1509–1520. https://doi.org/10.1007/s00216-020-02427-9

[49] Xu J, Wang K, Zu S-Z, Han B-H, Wei Z (2010) Hierarchical nanocomposites of polyaniline nanowire arrays on graphene oxide sheets with synergistic effect for energy storage. ACS Nano 4:5019–5026. https://doi.org/10.1021/nn1006539

[50] Ricciardi R, Auriemma F, Gaillet C, De Rosa C, Lauprêtre F (2004) Investigation of the crystallinity of freeze/thaw poly(vinyl alcohol) hydrogels by different techniques. Macromolecules 37:9510–9516. https://doi.org/10.1021/ma048418v